

SPITZER/MIPS 24 μm DETECTION OF PHOTOEVAPORATING PROTOPLANETARY DISKS

ZOLTAN BALOG^{1,2}, G. H. RIEKE¹, KATE Y. L. SU¹, JAMES MUZEROLLE¹, ERICK T. YOUNG¹

Draft version July 6, 2018

ABSTRACT

We present 24 μm images of three protoplanetary disks being photoevaporated around high mass O type stars. These objects have “cometary” structure where the dust pulled away from the disk by the photoevaporating flow is forced away from the O star by photon pressure on the dust and heating and ionization of the gas. Models of the 24 μm and 8 μm brightness profiles agree with this hypothesis. These models show that the mass-loss rate needed to sustain such a configuration is in agreement with or somewhat less than the theoretical predictions for the photoevaporation process.

Subject headings: circumstellar matter — stars: protoplanetary disks — stars: formation

1. INTRODUCTION

The discovery of “proplyds” in Orion (e.g. O’dell et al. 1993; O’dell & Wen 1994) let us image directly protoplanetary disks and study their structure. It also led to a number of theoretical studies of the photoevaporation of disks by external radiation fields from neighboring hot stars (Johnstone et al. 1998; Richling & Yorke 1998, 2000; Matsuyama et al. 2003; Hollenbach & Adams 2004; Throop & Bally 2005). Many of these studies predict behavior that agrees well with the proplyd properties. The proplyds have been observed intensely, for example through detection of associated molecular hydrogen (Chen et al. 1998) and high resolution measurements in the mid-infrared (Smith et al. 2005).

Deeper infrared observations can provide additional constraints for proplyd models. At 24 μm , the resolution of *Spitzer* is sufficient to identify and perhaps resolve such objects at distances up to a few kpc. At longer wavelengths, the resolution of *Spitzer* is too low to resolve these objects, and they will be lost in the confusion of the surrounding emission by interstellar material.

The predicted characteristics of an evaporating disk in the ~ 2 to 50 AU 24 μm -emitting zone differ substantially among the studies (Johnstone et al. (1998); Richling & Yorke (2000); Hollenbach & Adams (2004); Matsuyama et al. (2003)). However, the calculations do generally agree that the process occurs on a time scale of $\sim 1 - 3 \times 10^5$ years. As a result, one might expect to observe a wide range of consequences of disk evaporation. For stars that have dwelt close to an O star since their formation, we might find severely truncated disks and possibly reduced output in the 24 μm band. However, if the stellar velocities within a young stellar cluster are random, a star might enter the intense radiation field of an O star and begin the erosion of its disk well after its formation. A system that has just entered an O star radiation field is likely to be anomalously bright at 24 μm because dust grains that would normally be shielded from the ambient ultraviolet photons in the

optically thick disk are being torn from it by the evaporating gas and exposed to this field. Richling & Yorke (1998) calculate that the nominal disk emission at 24 μm may be boosted more than an order of magnitude for some stages in the evaporation process. This paper describes three systems that are in this dramatic process of early disk evaporation.

2. OBSERVATIONS

Our MIPS observations are taken in scan map mode and typically cover an area of 0.5-1 square degree. The raw data are converted to calibrated images with the instrument team Data Analysis Tool (DAT) (Gordon et al. 2005). Point source detection limits are as faint as ~ 0.4 mJy, although they can be higher in regions with significant variations in the infrared background. More details on the methods for reducing the data (including a description of the IRAC data reduction) can be found in papers describing the ensemble of infrared sources in the three clusters that are the subject of this paper: IC 1396 (Sicilia-Aguilar et al. 2006), NGC 2244 (Balog et al. in preparation), and NGC 2264 (Teixeira et al. 2006).

In our full GTO program, we have mapped several regions including a total of about twenty O stars. Based on a hypothesis that an evaporating disk might have a cometary appearance at 24 μm , with a photon-pressure-driven tail extending radially outward from the O star, we inspected these twenty regions. Three clear examples were found, illustrated in Figure 1, with their positions and integrated flux densities given in Table 1. We found no additional sources with tails extending in other directions. A simple and very conservative estimate of the probability of the three sources being chance alignments can be based on the fact that their tails are all within 10° of radial. This calculation would imply a probability of only about 10^{-4} that the alignments are random. This estimate ignores the unique morphology of these three sources, so the likelihood is even lower that they are randomly occurring phenomena.

The position of the head of each “comet” coincides with a 2MASS and IRAC point source. The sizes of the objects are similar to the cometary clouds of photoevaporating globulae found in Carina by Smith et al. (2004) but the near IR point sources at the positions of the “comet” heads indicate that they contain stars. No extended structures are observed at wavelengths

¹ Steward Observatory, University of Arizona, 933 N. Cherry Av. Tucson, AZ, 85721; zbalog@as.arizona.edu, grieke@as.arizona.edu, ksu@as.arizona.edu, jamesm@as.arizona.edu, eyoung@as.arizona.edu

² on leave from Dept of Optics and Quantum Electronics, University of Szeged, H-6720 Szeged Hungary

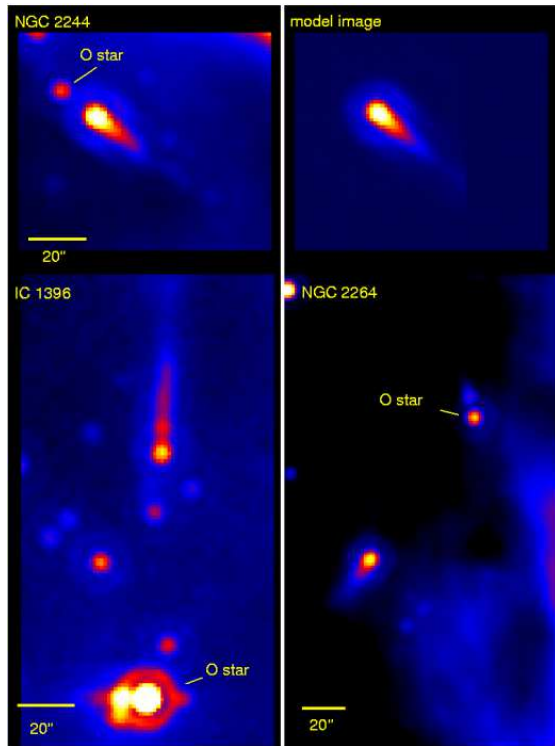


FIG. 1.— The three evaporating protoplanetary disks together with the modeled $24 \mu\text{m}$ image for the source in NGC 2244. The orientation of each image is north up and east toward the left. The upper right panel is the model $24 \mu\text{m}$ image for the tail in NGC 2244.

shorter than $24 \mu\text{m}$. The only exception is the source in NGC2244 where the $8 \mu\text{m}$ image also shows a similar cometary feature. The brightness (Table 1) and the infrared color of the near infrared objects in the heads indicate that they are stars with masses around $0.5 M_{\odot}$ - $1.0 M_{\odot}$. These mass estimates probably have large errors because a significant spread of ages is measured in each cluster.

Table 1. shows the basic parameters of the systems: the cluster to which they belong, the position of the head, the 2MASS K magnitude of the source in the head, the ionizing source and its age, the measured 8 and $24 \mu\text{m}$ flux densities including the tail, the length of the tail, the calculated total dust mass and the mass loss rate.

3. ANALYSIS AND MODELING

Our analysis is based on the hypothesis that the “cometary” tails represent dust entrained in gas evaporating from the working surface of the protoplanetary disk and being ejected away from the nearby O-type star. Richling & Yorke (1998) show theoretical calculations of the early stages of the process that are compatible with this possibility. Once the dust has been pulled from the disk, the smallest particles (radii $\ll 0.01 \mu\text{m}$) will be stochastically heated and some may be destroyed quickly. Small particles (radii $< 1000 \mu\text{m}$) will be blown away from the O star by photon pressure, or dragged away by the gas and will re-emit the absorbed UV energy in the thermal infrared.

The mid-infrared brightnesses of our three objects are similar to those of the Orion proplyds, corrected for dis-

tance (Smith et al. 2005). Only the system in NGC 2244 shows slightly extended structure at $8 \mu\text{m}$; the other two are point-like in the $8 \mu\text{m}$ images. The fact that all the tails are much brighter at $24 \mu\text{m}$ suggests that small grains (size less than $0.1 \mu\text{m}$) are the dominant emitters, assuming that the grains reach their equilibrium temperatures. To understand the structure of these tails, cuts with widths of $6''.23$ were made at 8 and $24 \mu\text{m}$ along the symmetric axis of the tail centered at the O star. The background values were estimated using the area above and below the tail and subtracted off. The surface brightness profiles are displayed in Figures 2, 3 and 4.

3.1. Basic Model and Parameters

To model the emission of the cometary tails we use the same model that Su et al. (2005) used for the extended Vega debris disk. This model considers the behavior of dust grains being blown away from a luminous central star by radiation pressure to form an extended outflow disk. It should apply generally for outward flows with a constant number density radially ($n(r) \sim \text{constant}$). To adapt the model to the current situation, we assume that the cometary outflow emerges from the disk (comet “head”) position. The remaining parameters are the dust properties (composition and grain sizes), the outer radius of the tail, and the angle that the line joining the O star and the head along the tail makes with respect to the plane of the sky (0° means the tail is pointed away from the O star exactly on the plane of sky). The emission from the tail is computed based on the equilibrium dust temperatures assuming the tail is optically thin (no stochastic heating is included). A series of model images was computed using different parameters, convolved with the *Spitzer* PSFs to match the observed resolutions, and then we extracted radial cuts for comparisons.

We first explored how the observed profiles of the tails vary with different grain sizes and angles to the plane of the sky. To simplify the modeling, we assumed the grains are astronomical silicates and have a uniform size (radius of a). The modeled $24 \mu\text{m}$ profiles basically fade rapidly as the grain sizes increase. This is because large grains have colder temperatures than small ones if they are at the same distance from the radiating source; as a result, the expected emission at $24 \mu\text{m}$ drops significantly, making a shorter observable tail. A similar characteristic is seen while varying the angles with respect to the plane of the sky, because even though the projected distance (on the plane of the sky) remains the same, the actual distance between the tail and the O star increases as the angle increases, resulting in colder dust temperatures and a shorter observable tail. In general, this simple model is degenerate between the sizes of grains and the actual angles of the tail with respect to the plane of the sky. However for the three systems discussed here, models based on grains larger than $\sim 1 \mu\text{m}$ come short of the observed tail lengths, and hence cannot fit the data even assuming the tails are on the plane of the sky. Without other data to constrain the model parameters, hereafter we assume the observed tails are exactly on the plane of the sky, for simplicity. This assumption is reasonable given the selection bias that they would be more difficult to recognize at other angles.

The Tail in NGC 2244: The tail in NGC 2244 is powered by the O5 V star HD46150, which we represent with

TABLE 1
THE PHYSICAL AND MODEL PARAMETERS OF THE EVAPORATING DISKS AND TAILS

Cluster	Position [J2000.0]	K [mag]	ionizing source	age* [Myr]	F_8 [mJy]	F_{24} [mJy]	Δl [pc]	\dot{M}_d^\dagger M_\odot	\dot{M}^\ddagger M_\odot/yr
NGC 2244	06:31:54.68 04:56:25.0	13.53	HD46150	4	1.5 ± 0.2	77 ± 10	0.22	$3 \times 10^{-8} - 9 \times 10^{-6}$	$1.4 \times 10^{-9} - 4.4 \times 10^{-7}$
IC 1396	21:38:57.09 57:30.46.5	13.18	HD206267	3	2.3 ± 0.1	23 ± 5	0.21	$5 \times 10^{-9} - 2 \times 10^{-6}$	$2.4 \times 10^{-10} - 7.7 \times 10^{-8}$
NGC 2264	06:41:01.92 09:52:39.0	13.65	S Mon	4	2.5 ± 0.1	78 ± 10	0.12	$4 \times 10^{-8} - 1 \times 10^{-5}$	$3.4 \times 10^{-9} - 1.1 \times 10^{-6}$

*HD46150 (Ogura & Ishida 1981), HD206267 (Heske, A. & Wendker 1985), S Mon (Walker 1956)

† Dust mass ranges from the observed dust mass using small ($\sim 0.01 \mu\text{m}$) grains based on the $24 \mu\text{m}$ profile (lower bound) and total mass integrating up to 1 mm size (upper bound).

‡ Mass loss rate is computed assuming a velocity of 10 km/s and a gas-to-dust mass ratio of 100.

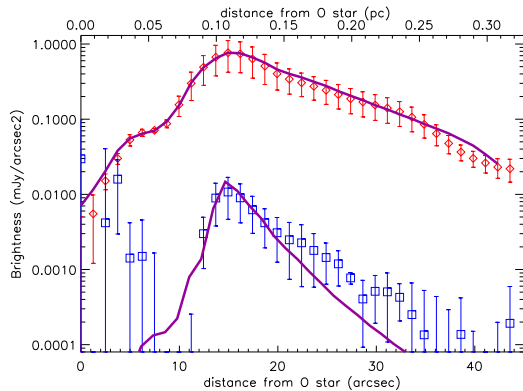


FIG. 2.— The brightness distribution of the tail in NGC 2244 with diamonds for the data at $24 \mu\text{m}$ and squares at $8 \mu\text{m}$, centered at the position of the O5 V star. The contribution of the O star has been taken out by PSF subtraction. The $8 \mu\text{m}$ profile within $8''$ from the O star is contaminated by the residual of the O star. The best-fit model is shown with the solid lines.

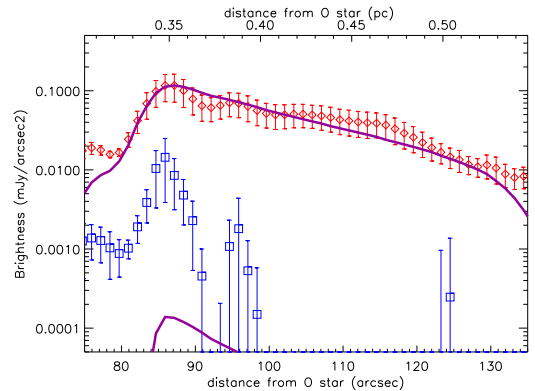


FIG. 3.— The brightness distribution of the tail in IC 1396. Symbols used are the same as Figure 2.

a blackbody of 42,000 K and $12 R_\odot$ located at a distance of 1.5 kpc. As shown in Figure 1, among the three systems this tail is the closest to the O star with a projected distance of ~ 0.1 pc (therefore the warmest). A tail composed of $a=0.03 \mu\text{m}$ grains produces a simultaneously good fit to the profiles at 8 and $24 \mu\text{m}$. Models with other grain sizes can also produce good fits to the $24 \mu\text{m}$ profile, but the expected emission at $8 \mu\text{m}$ is either much lower than the observed flux (for $0.03 < a < 0.3$), or much higher for ($a < 0.03 \mu\text{m}$). The best fit profiles are shown in Figure 2 as solid lines. The tail extends from 0.1 to 0.32 pc ($\Delta l \sim 0.22$ pc) from the O star, with a total observed dust mass of $\sim 3 \times 10^{-8} M_\odot$. The total model emission of the whole system is ~ 74 mJy at $24 \mu\text{m}$ and ~ 0.5 mJy at $8 \mu\text{m}$.

The Tail in IC 1396: The distance of IC 1396 is ~ 835 pc, much closer than NGC 2244. However, the projected distance between the disk and the O6 V star HD206267 is the largest (0.35 pc) with the longest observed angular tail length (0.35-0.56 pc, $\Delta l \sim 0.21$ pc) among the three systems. The tail also appears to be clumpy (see Figure 1), although this could also be due to a chance alignment with an unrelated source. As in the NGC 2244 object, a tail composed of $a \lesssim 0.01 \mu\text{m}$ grains can provide satisfactory fits to the observed $24 \mu\text{m}$ profile, but it cannot reproduce the flux at $8 \mu\text{m}$. One possible explanation is there exists a population of very small grains ($a \sim 10$

\AA) in the disk that are stochastically heated; therefore, the resultant emission spectrum would shift to shorter wavelengths producing more $8 \mu\text{m}$ flux than the emission spectrum using the thermal equilibrium temperature (e.g., Figure 8.12 in Kruegel 2003). The dust mass contribution from this very small grain population should be small. Therefore, the dust mass derived from our simple model, $\sim 5 \times 10^{-8} M_\odot$, is a reasonable estimate. The total model emission at $24 \mu\text{m}$ is ~ 19 mJy and < 0.01 mJy at $8 \mu\text{m}$.

The Tail in NGC 2264: The cluster NGC 2264 is located ~ 800 pc away, similar to IC 1396. The star powering the tail, S Mon, is slightly cooler than the other two cases, O7 Ve; therefore a blackbody of 38,000 K and $9 R_\odot$ was used. The disk is also farther away from the O star, 0.3 pc, with the shortest tail length (0.32-0.44 pc, $\Delta l \sim 0.12$ pc) among these three systems. In addition, the contrast between the head (profile within $6''$ from the head position) and the tail is much larger than the other two cases (see Figure 4). Therefore, similar models used to fit the tails in NGC 2244 and IC 1396 cannot obtain a good fit to the observed $24 \mu\text{m}$ profile. An additional unresolved point source at the position of the disk is added to fit the profile. Our models are also too faint at $8 \mu\text{m}$. The behavior at both wavelengths suggests the presence of a population of very small grains that are rapidly destroyed. The models with grains with $a < 0.01 \mu\text{m}$ can produce good fits to the rest of the $24 \mu\text{m}$ profile. The total observed dust mass is $\sim 4 \times 10^{-8} M_\odot$, and the total emission at $24 \mu\text{m}$ is ~ 66 mJy and $\ll 0.1$ mJy at $8 \mu\text{m}$.

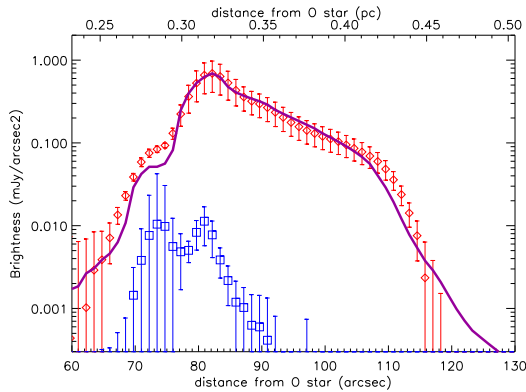


FIG. 4.— The brightness distribution of the tail in NGC 2264. Symbols used are the same as Figure 2.

3.2. Implications

Although small grains ($a \sim 0.01 \mu\text{m}$) are responsible for most of the emission at $24 \mu\text{m}$, larger “invisible” grains may contribute significantly to the total dust mass in the tail. To estimate the mass, we assume that the grains have a size distribution similar to the interstellar medium, $N(a) \propto a^{-3.5}$, as is also expected for grains undergoing collisional cascades in protoplanetary disks (Dohnanyi 1969; Tanaka et al. 1996). The total dust mass in the tail is then $M_{\text{tot}} \propto \int \frac{4}{3}\pi a^3 N(a) da \propto \int a^{-0.5} da \propto a^{0.5}$. Integrating between $0.01 \mu\text{m}$ and 1 mm (roughly the largest grain size that can be ejected by the radiation pressure of an O star) gives an upper limit to the total dust mass in the tail; values are listed in Table 1.

We can also estimate the mass loss rate in the photoevaporating disks given the velocity of the flow in the cometary tails. Following the equation given in Su et al. (2005), the terminal velocity ranges from ~ 10 to 100 km s^{-1} for a typical O-type star (luminosity of $10^6 L_{\odot}$ and mass of $50 M_{\odot}$) and grains with sizes of $1\text{--}0.01 \mu\text{m}$, assuming negligible gas drag effects. The presence of gas in the tail will result in lower velocities. However, heating and ionization accelerate gas to speeds of $3\text{--}20 \text{ km s}^{-1}$ (Johnstone et al. 1998; Bally et al. 1998) and these flows entrain dust.

Although the flow velocity is hard to determine accurately, our estimate for the mass loss rate is robust because it depends on the product of the velocity and the gas to dust ratio which are roughly inversely correlated to each other. For a normal gas to dust ratio (100:1) the bulk velocity of the dust and gas mixture is on the order of 10 km s^{-1} . If the gas to dust ratio deviates from the standard value (the effect of gas decreases) the bulk velocity will approach the terminal velocity. Although the outflow velocity of material will increase the total calculated mass loss will remain approximately the same since

the lower gas to dust ratio will result in lower total mass, hence a lower mass loss rate.

The X-ray observations of these O stars indicate significant stellar winds ($L_x = 10^{32.4} \text{ erg/s}$ for S Mon, Simon & Dahm 2005; $L_x = 10^{32.5} \text{ erg/s}$ for HD46150, Walborn et al. 2002; and a bright ROSAT source for HD206267, Berghoefer et al. 1996). The strong stellar winds would speed up the outflow from the disk if the disk was very close to the O star (less than 0.01 pc). However, such winds should be only a secondary effect at the distances of these objects from the stars.

We can place lower and upper limits on the mass loss rate, corresponding to the observed grain sizes and to the full size range up to $1000 \mu\text{m}$. We take a typical gas-to-dust mass ratio of 100 and a velocity of 10 km/s . The range of mass loss rate is 1.4×10^{-10} to $4.4 \times 10^{-8} M_{\odot} \text{ yr}^{-1}$, 2.4×10^{-11} to $7.7 \times 10^{-9} M_{\odot} \text{ yr}^{-1}$, and 3.4×10^{-10} to $1.1 \times 10^{-7} M_{\odot} \text{ yr}^{-1}$ for the tails in NGC 2244, IC 1396 and NGC 2264, respectively. To first order, the upper limits of the derived mass loss rates are somewhat less than the predictions by the photoevaporation models, $\sim 1 - 6 \times 10^{-7} M_{\odot} \text{ yr}^{-1}$ at $0.3 - 0.1 \text{ pc}$ from the UV energy source (Richling & Yorke 1998; Yorke 2004), and the lower limits are much less than these expectations.

4. CONCLUSIONS

We report the detection of three photoevaporating disks with cometary tails around high-mass stars in *Spitzer*/ $24 \mu\text{m}$ images. Their observed brightnesses and morphologies agree well with a model where the dust is entrained in the evaporating gas and pulled from the disk. Once exposed to the O star radiation field, a structure like a comet tail grows, with dust and gas streaming away from the O star under the influence of its radiation pressure on the dust and heating and ionization of the gas. We have roughly estimated the evaporation mass loss rate from our observations and find an upper limit in reasonable agreement with or somewhat lower than theoretical expectations. Further observations of these systems should be able to improve our understanding of the evaporation process substantially.

We thank the referee, John Bally for suggestions that greatly improved the manuscript. This work is based on observations made with the Spitzer Space Telescope, which is operated by the Jet Propulsion Laboratory, California Institute of Technology, under NASA contract 1407. Support for this work was provided by NASA through contract 1255094, issued by JPL/Caltech. ZB received support from Hungarian OTKA Grants TS049872, T042509 and T049082.

REFERENCES

- Bally, J., Sutherland, R. S., Devine, D., & Johnstone, D. 1998 AJ, 116, 293
 Berghoefer, T. W., Schmitt, J. H. M. M., & Cassinelli, J. P. 1996, A&AS, 118, 481
 Chen, H., Bally, J., O’dell, C. R., McCaughrean, M. J., Thompson, R. L., Rieke, M., Schneider, G., & Young, E. T. 1998, ApJ, 492, L173+
 de La Fuente, E., Rosado, M., Arias, L., & Ambrocio-Cruz, P. 2003, Revista Mexicana de Astronomia y Astrofisica, 39, 127
 Dohnanyi, J. W. 1969, J. Geophys. Res., 74, 2531
 Gordon, K. D., et al. 2005, PASP, 117, 503
 Henney, W. J., O’Dell, C. R., Meaburn, J., Garrington, S. T., & Lopez, J. A. 2002, ApJ, 566, 315
 Heske, A. & Wendker, H. J. 1985 A&A, 149, 199

- Hollenbach, D. & Adams, F. C. 2004, in ASP Conf. Ser. 324: Debris Disks and the Formation of Planets, 168–+
- Johnstone, D., Hollenbach, D., & Bally, J. 1998, *ApJ*, 499, 758
- Kruegel, E. 2003, *The physics of interstellar dust (The physics of interstellar dust, by Endrik Kruegel. IoP Series in astronomy and astrophysics, ISBN 0750308613. Bristol, UK: The Institute of Physics, 2003.)*
- Matsuyama, I., Johnstone, D., & Murray, N. 2003, *ApJ*, 585, L143
- Meaburn, J., Graham, M. F., & Redman, M. P. 2002, *MNRAS*, 337, 327
- O'dell, C. R. & Wen, Z. 1994, *ApJ*, 436, 194
- O'dell, C. R., Wen, Z., & Hu, X. 1993, *ApJ*, 410, 696
- Ogura, K. & Ishida, K. 1981, *PASJ*, 33, 149
- Richling, S. & Yorke, H. W. 1998, *A&A*, 340, 508
- . 2000, *ApJ*, 539, 258
- Sicilia-Aguilar, A. et al. 2006, *ApJ*, 638, 897
- Simon, T. & Dahm, S. E. 2005, *ApJ*, 618, 795
- Smith, N., Bally, J., Shuping, R. Y., Morris, M., & Kassis, M. 2005, *AJ*, 130, 1763
- Smith, N., Barbá, R. H. & Walborn, N. R. 2004, *MNRAS*, 351, 1457
- Su, K. Y. L., et al. 2005, *ApJ*, 628, 487
- Tanaka, H., Inaba, S., & Nakazawa, K. 1996, *Icarus*, 123, 450
- Teixeira, P. S. et al. 2006, *ApJ*, 636, L45
- Throop, H. B. & Bally, J. 2005, *ApJ*, 623, L149
- Vasconcelos, M. J., Cerqueira, A. H., Plana, H., Raga, A. C., & Morisset, C. 2005, *AJ*, 130, 1707
- Walborn, N. R. et al. 2002, *AJ*, 123, 2754
- Walker, M. F. 1956, *ApJS*, 2, 365
- Yorke, H. W. 2004, in *Revista Mexicana de Astronomía y Astrofísica Conference Series*, 42–45